Numerical simulation of the hydrodynamics and water exchange in Sansha Bay

Hongyang Lin[a,b], Zhaozhang Chen[a,*], Jianyu Hu[a], Andrea Cucco[c], Jia Zhu[a], Zhenyu Sun[a], Lingfeng Huang[b]

[a] *State Key Laboratory of Marine Environmental Science, College of Ocean and Earth Sciences, Xiamen University, Xiamen, Fujian 361102, China*
[b] *College of the Environment and Ecology, Xiamen University, Xiamen, Fujian 361102, China*
[c] *Institute for Coastal Marine Environment, CNR-IAMC, TorreGrande, 09170 Oristano, Italy*

ARTICLE INFO

ABSTRACT

A two-dimensional shallow water hydrodynamic finite element model (SHYFEM) was applied to Sansha Bay, Fujian, China. The model was used to investigate the hydrographic characteristics of the bay and in particular its water-exchange ability with the open sea. Comparisons between model output and observations indicate that the model is generally capable of reproducing the variability of water level and currents in the study region. Further analysis suggests that the magnitude of currents is larger in deep water areas such as channels, reaching approximately 1 m s^{-1}, whereas it is often less than 0.5 m s^{-1} in shallow water areas such as tidal flats. By contrast, the residual currents are much weaker, without a clear inward or outward direction. Seawater in deeper areas tends to exchange faster with the open sea compared to that in shallower regions. The half-exchange time of sea water is < 10 d along main channels, while it exceeds 30 d in bay heads. Model sensitivities suggest that (i) dredging of tidal flats increases the exchange rate of seawater near bay heads, (ii) increasing river runoff or opening up an extra passage can significantly increase the exchange rate locally yet slightly decrease it in other secondary bays.

1. Introduction

Sansha Bay, situated in the northeastern area of Fujian, China, is a semi-enclosed bay consisting of several secondary bays such as Baima Harbor, Yantian Harbor, Dongwuyang, Guanjingyang and Sanduao (see Fig. 1 for locations). Sansha Bay has a relatively large water area of approximately 675 km^2, but there is only one narrow gateway (i.e., Dongchong Channel) of approximately 3-km wide in the south bridging the bay and the outer waters (i.e., the Taiwan Strait). Due to such a geographical feature, Sansha Bay has historically been a natural sheltered bay (Wang et al., 2009). It is also a famous spawning ground of the large yellow croaker in China.

In recent years, water quality and ecosystem of Sansha Bay have been strongly affected by land-based pollution, coastal industries, aquaculture, and urbanization, resulting in severe habitat degradation (Wang et al., 2011; Wu et al., 2012; Sun et al., 2015). Previous studies have pointed out that dissolved inorganic nitrogen (DIN) and active phosphorus (AP) are the two primary factors inducing degraded water quality (Liu et al., 2003; Shen et al., 2014; Sun et al., 2015). Sources of DIN and AP have been attributed primarily to river inputs (including

massive untreated industrial and domestic sewage) and cage aquaculture (Cai, 2007; Shen et al., 2014; Sun et al., 2015). The increasing trend of DIN and AP in Sansha Bay is in turn becoming an important factor hindering the sustainable development of cage aquaculture (Cai, 2007). Therefore, ecological restoration in Sansha Bay is practically important and has attracted increasing attention from various communities.

In addition to regular ecological restoration schemes (e.g., Boesch et al., 2001), it is generally more efficient to propose appropriate physical restoration schemes based on the known hydrodynamic background. Better understanding of the hydrographic characteristics of Sansha Bay and its water-exchange ability with the open sea facilitates proposing the physical-based schemes in a more effective way. Given the limited observations, physical oceanographic aspects of Sansha Bay have not been well understood. Most previous studies focused on the tidal features or the effect of reclamation on channels (e.g., Wang et al., 2002; Ye et al., 2007).

Two cruises were conducted in Sansha Bay in order to collect newly in-situ observations: one in summer (August–September 2012) and the other in winter (January–March 2013). Cruise measurements included

---
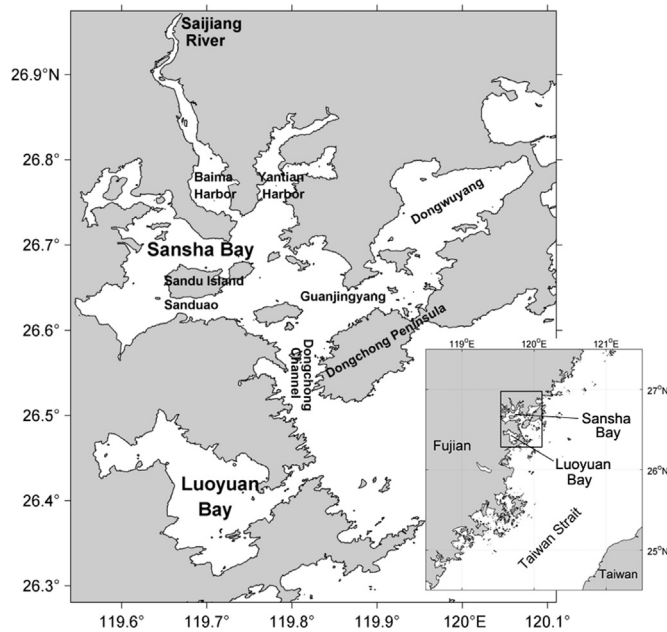
Fig. 1. Map of Sansha Bay with the main islands, harbors and channels labeled. The lower right inset shows the location of Sansha Bay.

temperature, salinity, currents, and time series of water level. Based on these observations, a preliminary understanding of the hydrographic/hydrodynamic features was obtained (Lin et al., 2016a). The interactions between tides and regional wind forcing were also investigated using measurements of water level and the contemporaneous wind fields (Lin et al., 2016b). Nevertheless, in-situ measurements are still rather limited and costly, which naturally calls for the need of developing a hydrodynamic model for Sansha Bay. The above-mentioned observations could also be used in model validation. The application of a robust hydrodynamic model can be useful in better understanding the regional oceanography and also in proposing more effective physical-based restoration schemes.

A two-dimensional hydrodynamic model was applied for Sansha Bay in this study, based on the shallow water hydrodynamic finite element model (SHYFEM) developed by Umgiesser et al. (2004). The model will be used to examine the hydrographic characteristics (e.g., variations of water level and currents) in Sansha Bay and its water-exchange ability with the outer waters (e.g., half-exchange time).

2. The numerical model

The SHYFEM was designed to simulate physical processes in lagoons, coastal seas, estuaries and lakes (Umgiesser et al., 2004; Umgiesser, 2009). The model uses the finite element technique and an effective semi-implicit scheme, making it particularly suitable to be applied in bays with complicated geography and bathymetry such as Sansha Bay. The finite element technique allows for more convenient increasing of the spatial resolution as needed in regions of particular interest, and the model is also capable of handling wetting and drying processes in a mass conserving way (Umgiesser et al., 2004). The model is also coupled with an advection and diffusion numerical module to simulate the transport of passive or active tracers induced by currents (Cucco and Umgiesser, 2006).

2.1. The model equations

The SHYFEM is particularly suited to be run in very shallow basins (Umgiesser et al., 2004) under strong influence of tides, so the water is normally assumed to be vertically well-mixed and hence ignores stratification. The set of hydrodynamic equations is then reduced to

the depth-averaged shallow water equations (e.g., Csanady, 1982). The momentum and continuity equations are:

$$\frac{\partial u}{\partial t} + u\frac{\partial u}{\partial x} + v\frac{\partial u}{\partial y} - fv = -g\frac{\partial \eta}{\partial x} - \frac{ru\sqrt{u^2 + v^2}}{H}$$

$$\frac{\partial v}{\partial t} + u\frac{\partial v}{\partial x} + v\frac{\partial v}{\partial y} + fu = -g\frac{\partial \eta}{\partial y} - \frac{rv\sqrt{u^2 + v^2}}{H}$$

$$\frac{\partial \eta}{\partial t} + \frac{\partial (uH)}{\partial x} + \frac{\partial (vH)}{\partial y} = 0$$

$$\tag{1}$$

where u and v are zonal and meridional components of velocity, respectively; η is sea surface elevation, H is the total water depth ($H = h + \eta$ with h being the mean depth), f is the Coriolis parameter, r is the bottom drag coefficient and g is the acceleration due to gravity.

The model is coupled with an advection and diffusion module which is used to describe the simulated current induced transport of a passive tracer P, which represents the concentration of a pollutant. The equation reads:

$$\frac{\partial P}{\partial t} + \frac{\partial UP}{\partial x} + \frac{\partial VP}{\partial y} = \frac{\partial}{\partial x}\left(HK_x\frac{\partial P}{\partial x}\right) + \frac{\partial}{\partial y}\left(HK_y\frac{\partial P}{\partial y}\right) + S$$

$$\tag{2}$$

where P denotes the concentration of a pollutant, U and V are the depth-integrated velocities (namely total or barotropic transports) in x- and y-directions, respectively, calculated by the hydrodynamic model, K_x and K_y are the coefficients of diffusivity, and S denotes the pollutant source per unit area and per unit time. The pollutants are assumed to be conservative materials in the model.

During ebb tide, the open boundary condition is given by $\frac{\partial P}{\partial t} + \vec{V} \cdot \vec{n} \frac{\partial P}{\partial n} = 0$, where $\vec{n}$ is the unit normal vector and $\vec{V}$ is the velocity vector. During flood tide, the open boundary condition is given by $P = C_0$, where C_0 is the background concentration.

2.2. The model setup

The finite element mesh specifically developed for Sansha Bay is shown in Fig. 2, representing the Sansha Bay, Luoyuan Bay (to the south of Sansha Bay) and their outer regions with triangular elements of different size and shape. The finite element technique allows the model to capture the complicated coastline more accurately, and also to increase the spatial resolution in areas of particular interest. A total of 21407 nodes and 37581 triangular cells were used to represent the model domain with higher spatial resolution, up to 10 m, in secondary bays.

In addition to the solid boundaries naturally formed by the bay-head coastlines of each secondary bay, the model also has an open southeastern boundary which is set to be a straight line connecting stations Tailu and Waicheng (Fig. 2a). The model bathymetry (Fig. 2a) was obtained by digitizing the nautical chart of Sansha Bay and Luoyuan Bay published in 2009. It is shown that the water depths in the vicinity of each bay head are typically less than 5 m. Parts of such areas are defined as tidal flats which are wet during high tide while are dry during low tide. The water depths at channels are relatively deep, reaching about 20–30 m, and it is the deepest at the bay mouth, exceeding 50 m.

The model starts to integrate from rest, i.e., at time $t = 0$, $u = v = \eta = 0$. The in-situ water-level time series at stations Tailu and Waicheng are used as open boundary conditions to drive the model. Since Sansha Bay is a relatively small near-enclosed bay, tidal forcing at the open boundary is much more important than other forcing such as the local winds. The good agreement between observations and model simulations, as will be shown below, proves that considering tides at the open boundary as the only model forcing is a
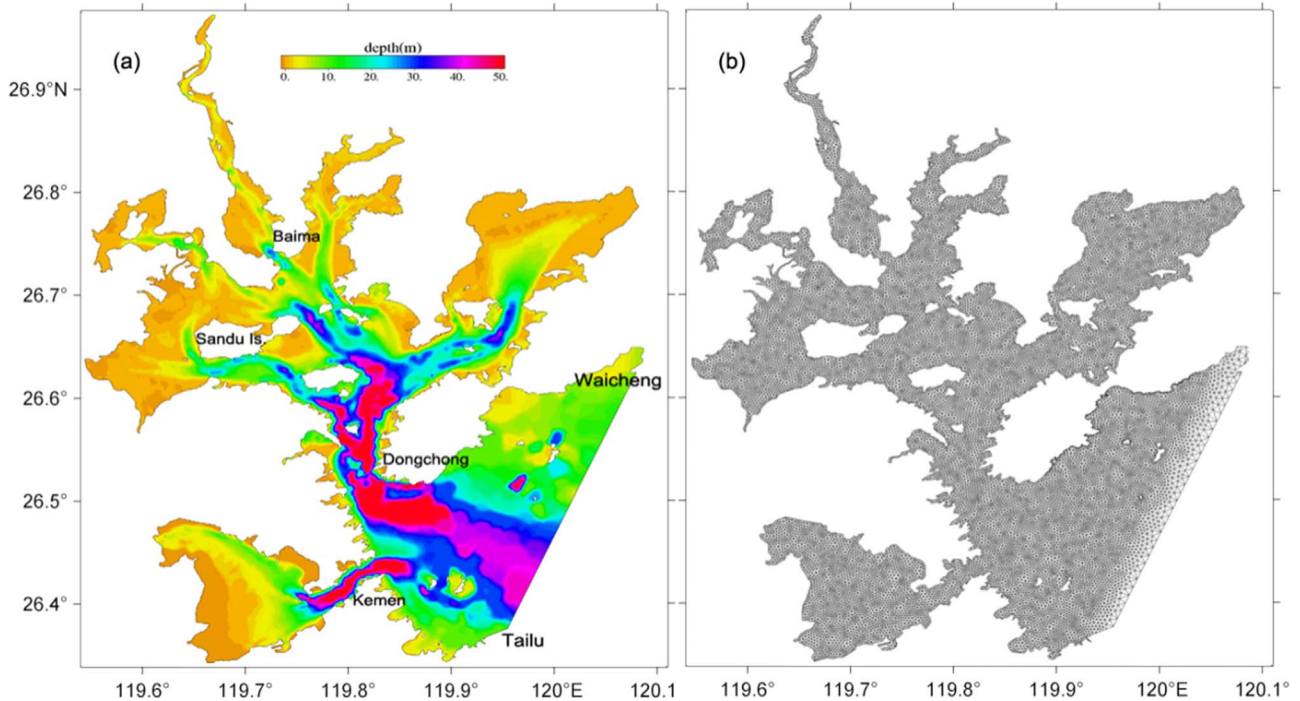
Fig. 2. (a) Bathymetry and (b) the model grids of the model domain.

pretty good approximation. The observed time series last for longer than a month at each station, both in summer and winter. Water levels at the straight line (open boundary) connected by the two stations are obtained by linear interpolation of the observed time series. A full slip boundary condition is applied at coastlines. Due to the relatively small domain, the model becomes stable after a spin up of about one tidal cycle and the output after that is used for model validation and further analysis. A fixed time step of 5 s has been used for the numerical simulation. The bottom drag coefficient r is set to be 0.0025, and the diffusivity coefficients K_x and K_y both equal to 30 m s^{-1}.

3. Model validation

The model integration was performed in summer and winter using the corresponding open boundary conditions, respectively. Since the spin up only lasts for about one tidal cycle, each model integration period was the same as the length of the observed water-level time series, and the model output after stability was used for model validation.

Only winter in-situ measurements (collected in January 2013), including water level and currents, are shown here to compare with the model output. Model validation for summer is not shown in order to shorten the length of the manuscript although the model performance is qualitatively similar in both seasons. The observations were collected in six water-level stations and six current stations (see Fig. 3 for locations).

The observed and simulated time series of water level are shown in Fig. 4, which reveals that Sansha Bay is clearly characterized by the regular semi-diurnal tide. It has a relatively large tidal range, reaching 6–7 m during spring tide. The water-level time series simulated by the model agree well with the observations in terms of both amplitude and phase. The observed and simulated time series of current speed and direction in spring tide are shown in Fig. 5. The comparisons suggest that the model is generally capable of reproducing the current field in the study area.

Two statistical metrics are introduced to measure the bias between the observations and model output more quantitatively: averaged absolute difference (AAD; Urrego-Blanco and Sheng, 2012) and γ^2
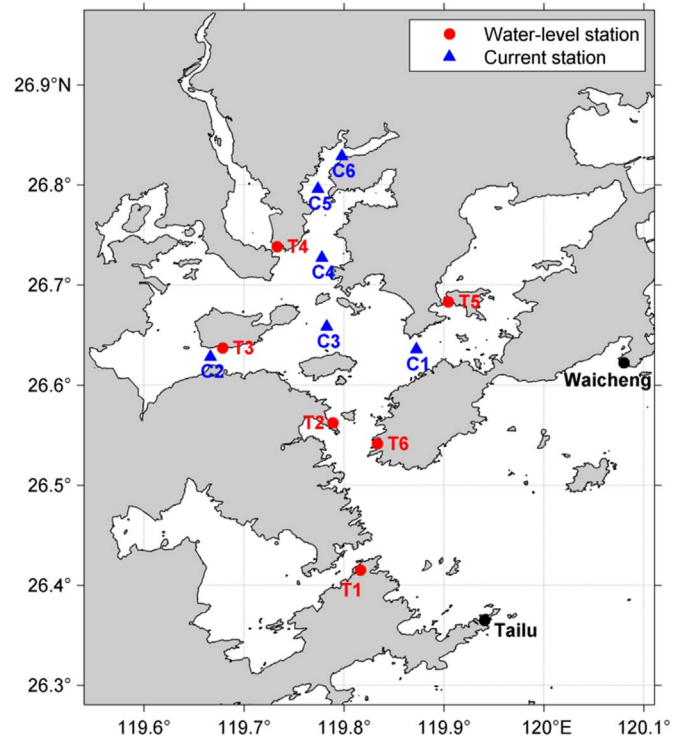
Fig. 3. Observation stations of water level (red dots) and current (blue triangles) of which the in-situ data are used for model validation. The black dots denote the two stations of which the measured water levels are used as open boundary conditions for the model. (For interpretation of the references to color in this figure legend, the reader is referred to the web version of this article.)

(Thompson and Sheng, 1997), which are defined as:

$$AAD = \frac{1}{N} \sum_{i=1}^{N} |O_i - M_i|$$

$$\gamma^2 = \frac{Var(O - M)}{Var(O)}$$
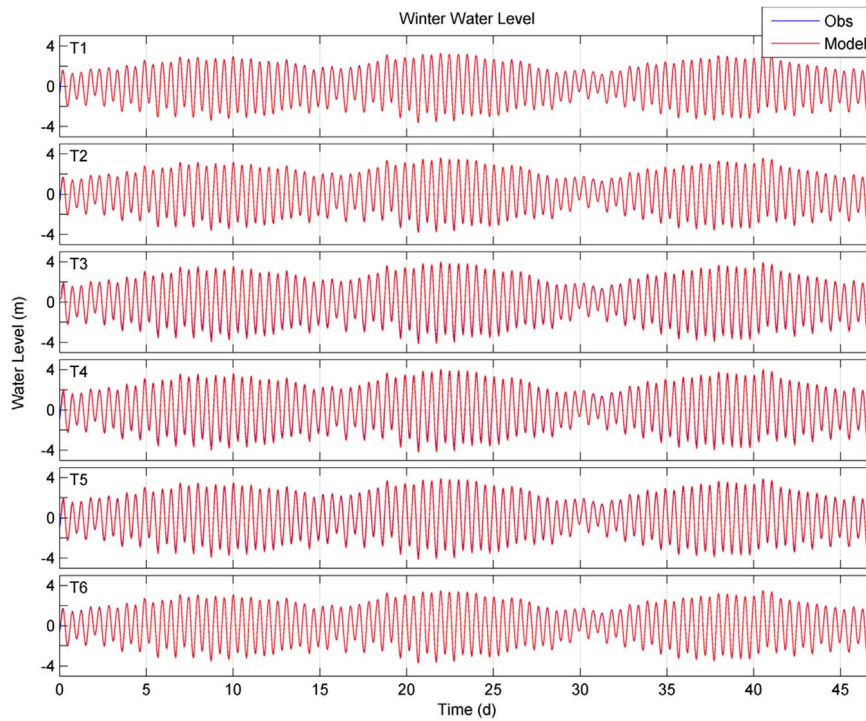
Fig. 4. Observed (blue) and simulated (red) time series of winter water level in the six stations. (For interpretation of the references to color in this figure legend, the reader is referred to the web version of this article.)
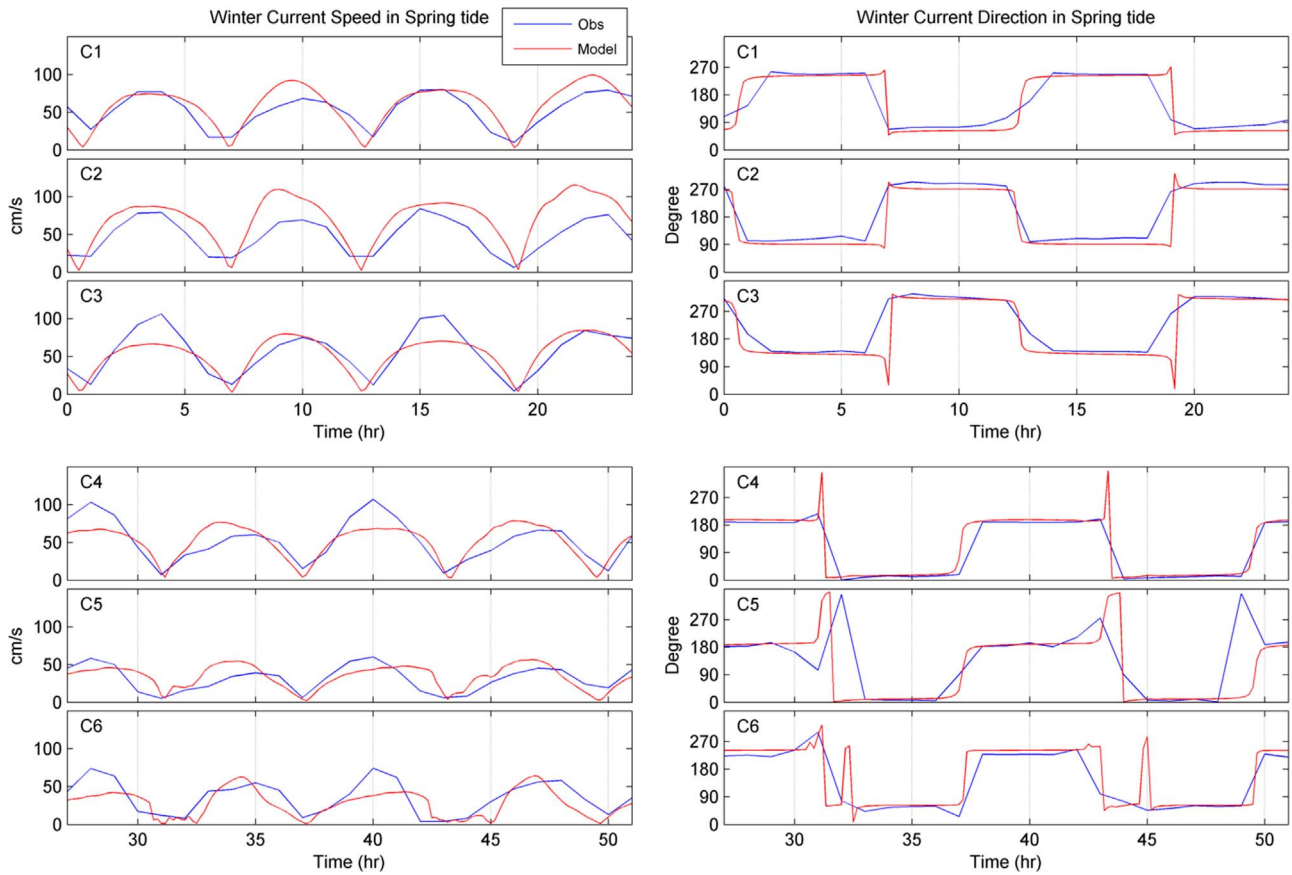
Fig. 5. Observed (blue) and simulated (red) time series of winter current speed (left panels) and current direction (right panels) during spring tide in the six stations. (For interpretation of the references to color in this figure legend, the reader is referred to the web version of this article.)
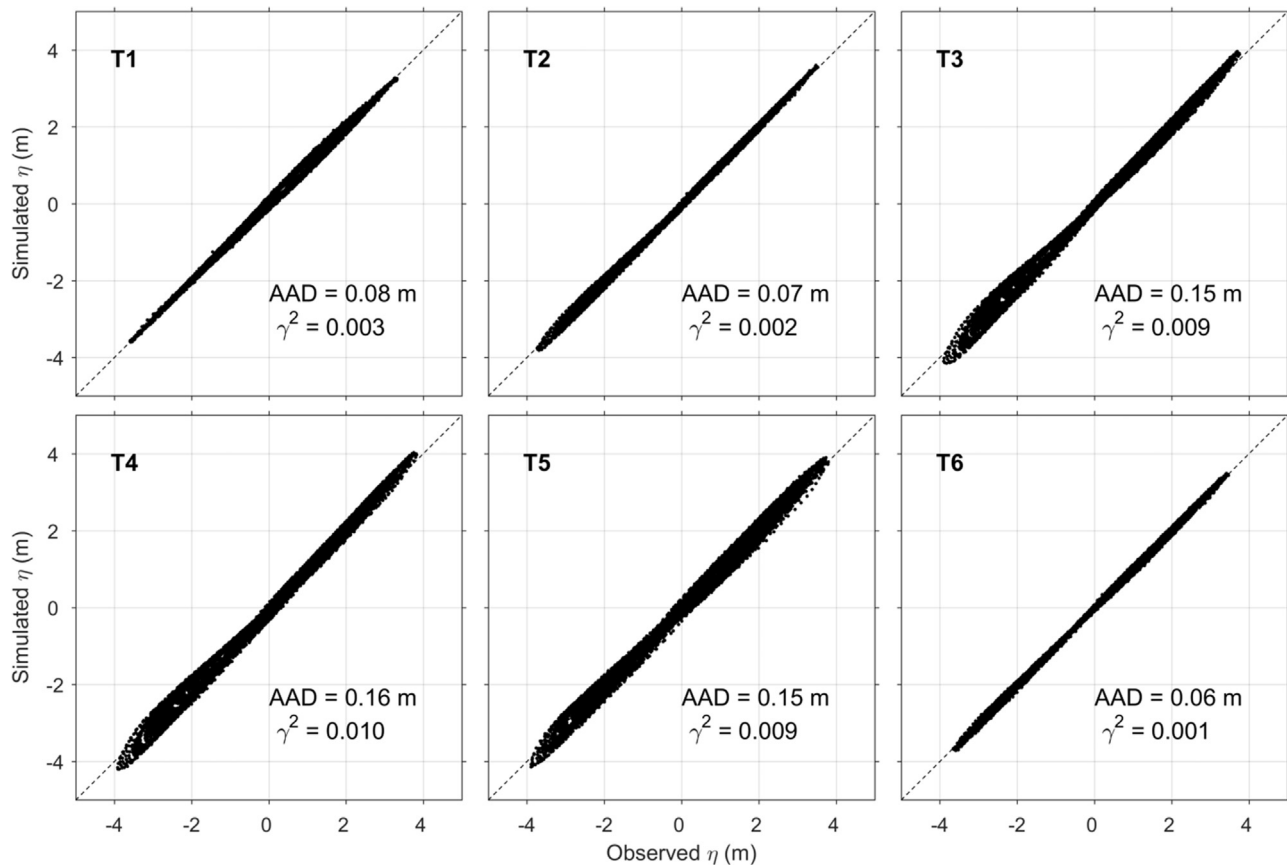
Fig. 6. Scatterplots of observed and simulated winter water levels in the six stations. The metrics of AAD and γ^2 are labeled for each station.

where O and M denote values from the observations and model simulations, respectively; subscript i denotes the ith time step with a total of N time steps; Var is the variance operator. AAD quantifies the mean error of model simulations and carries the unit of the variables being validated. However, it is not straightforward to directly assess model skill based on AAD values (Zhang and Sheng, 2013, 2015). By contrary, γ^2 is a nondimensional parameter that measures the fit of model output to observations. Generally higher model skill is accompanied by smaller values of γ^2 (Thompson and Sheng, 1997). Values of AAD and γ^2 will be calculated for water level, current speed and current direction for each station to evaluate the model performance.

Scatterplots of water levels show a close agreement between the observations and model simulations. The scattered points closely follow the diagonal line where observations equal simulations (Fig. 6). AAD values are mostly smaller than 0.15 m and more importantly γ^2 are all less than 0.01. This implies that the model is able to well reproduce water-level variability in Sansha Bay, be it in deep or shallow areas. In contrast, scatterplots of current speeds show much more scattered dots, which, nevertheless, still roughly follow the diagonal line (Fig. 7). Values of γ^2 are less than 0.5 except in C5 and C6 of which the water depth is shallower than 10 m (Fig. 2a). Scatterplots of current directions show two discrete groups of closely spaced dots around the diagonal line in each station (Fig. 7), suggestive of reversing flows induced by tides. Current direction is only considered when current speed is larger than 0.2 m s^{-1} to reduce direction ambiguity associated with rather weak flows. Unlike current speed, values of γ^2 for current direction are all less than 0.02. Scatterplots for velocities indicate that the model is generally capable of reproducing the velocity field in Sansha Bay, particularly the current direction.

There is still room for improvement in simulated current speeds, particularly in shallow regions. The less skillfulness in speed simulation is probably due to the non-differentiated drag coefficient r (see Eq. (1))

prescribed in the model, which is expected to vary with water depths. In addition, aquaculture cages are densely populated in Sansha Bay. So for a more realistic model setup, the drag coefficient is supposed to be prescribed as per the spatial distribution of cages, which will be exclusively investigated in a separate study.

In general, the model is able to simulate the water-level variability and the flow field in Sansha Bay, and hence the model output will be used for further analysis of the water exchange ability of Sansha Bay with the open sea.

4. Hydrodynamic characteristics of Sansha Bay

The model validation shown in the previous section suggests that the two-dimensional model is generally capable of reproducing the hydrodynamic features of Sansha Bay. The model output is thus used to further investigate the hydrodynamic features of Sansha Bay, focusing on its water-exchange ability with the adjacent open sea.

4.1. Flow field

The current fields for flood tide, ebb tide and the corresponding residual current during spring tide in Sansha Bay are shown in Fig. 8. During flood tide, sea water flows from the outer bay into the inner bay primarily along the main channels (Fig. 8a). Stronger current velocity is seen in deeper areas such as the main channels, with a magnitude of approximately 1 m s^{-1}. The current velocity along the narrow Dongchong Channel even exceeds 1.5 m s^{-1}. Weaker velocity with a magnitude less than 0.5 m s^{-1} exists in shallower areas extending from tidal flats to the bay heads. Oppositely, sea water flows out along the main channels during ebb tide (Fig. 8b). The ebb current velocity is stronger than the flood current velocity in magnitude, normally with a magnitude exceeding 1 m s^{-1}. Similarly, the ebb current velocity in the
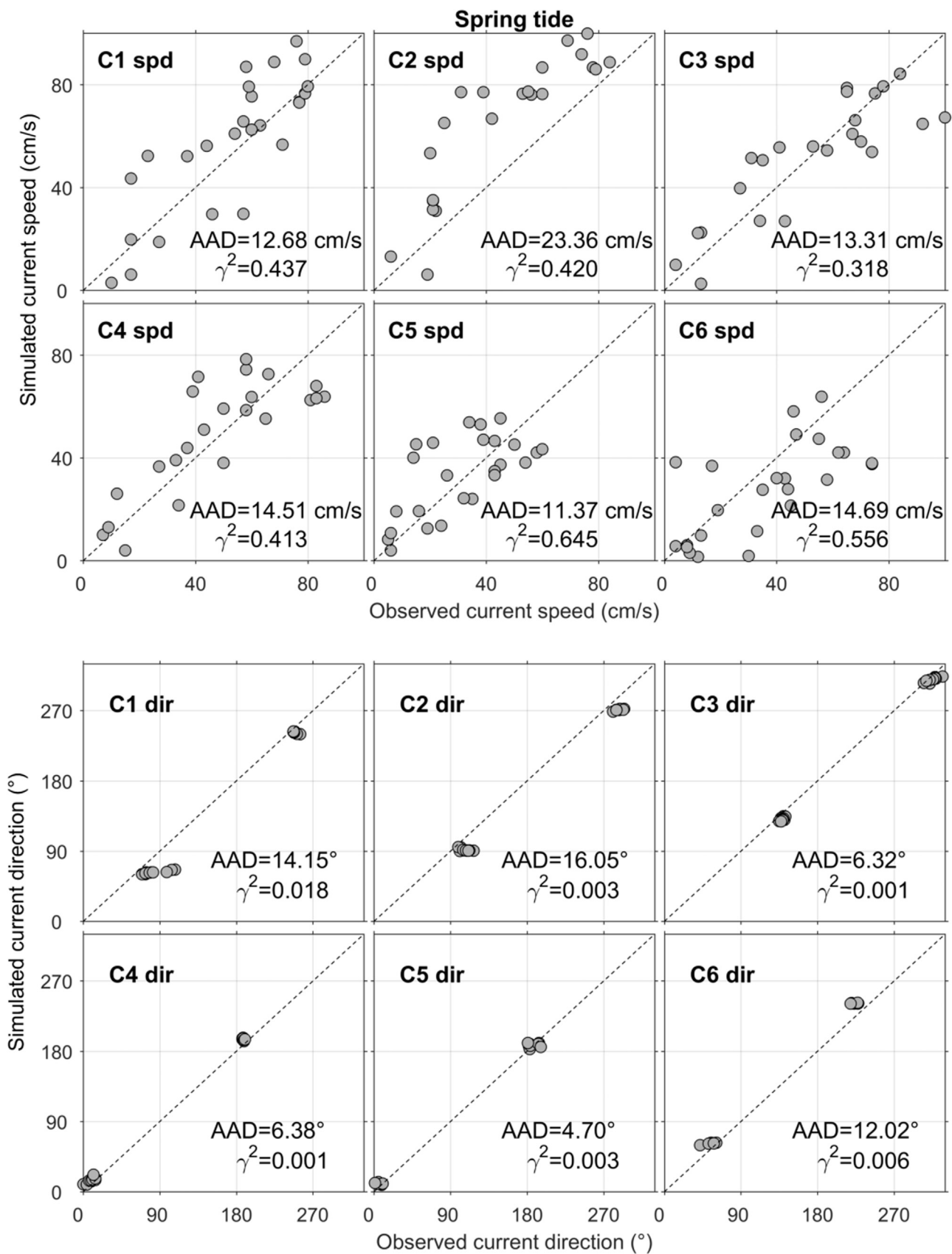
Fig. 7. Scatterplots of observed and simulated winter currents during spring tide in the six stations. Upper two rows: current speed; lower two rows: current direction.

vicinity of Dongchong Channel exceeds 1.5 m s⁻¹. The residual flow field of Sansha Bay exhibits a relatively complicated, multi-eddy structure (Fig. 8c), with a current velocity generally weaker than

0.05 m s⁻¹. The residual current velocity is slightly higher in several areas immediately close to the coastline, probably due to larger differences of flood and ebb currents in such complicatedly shaped
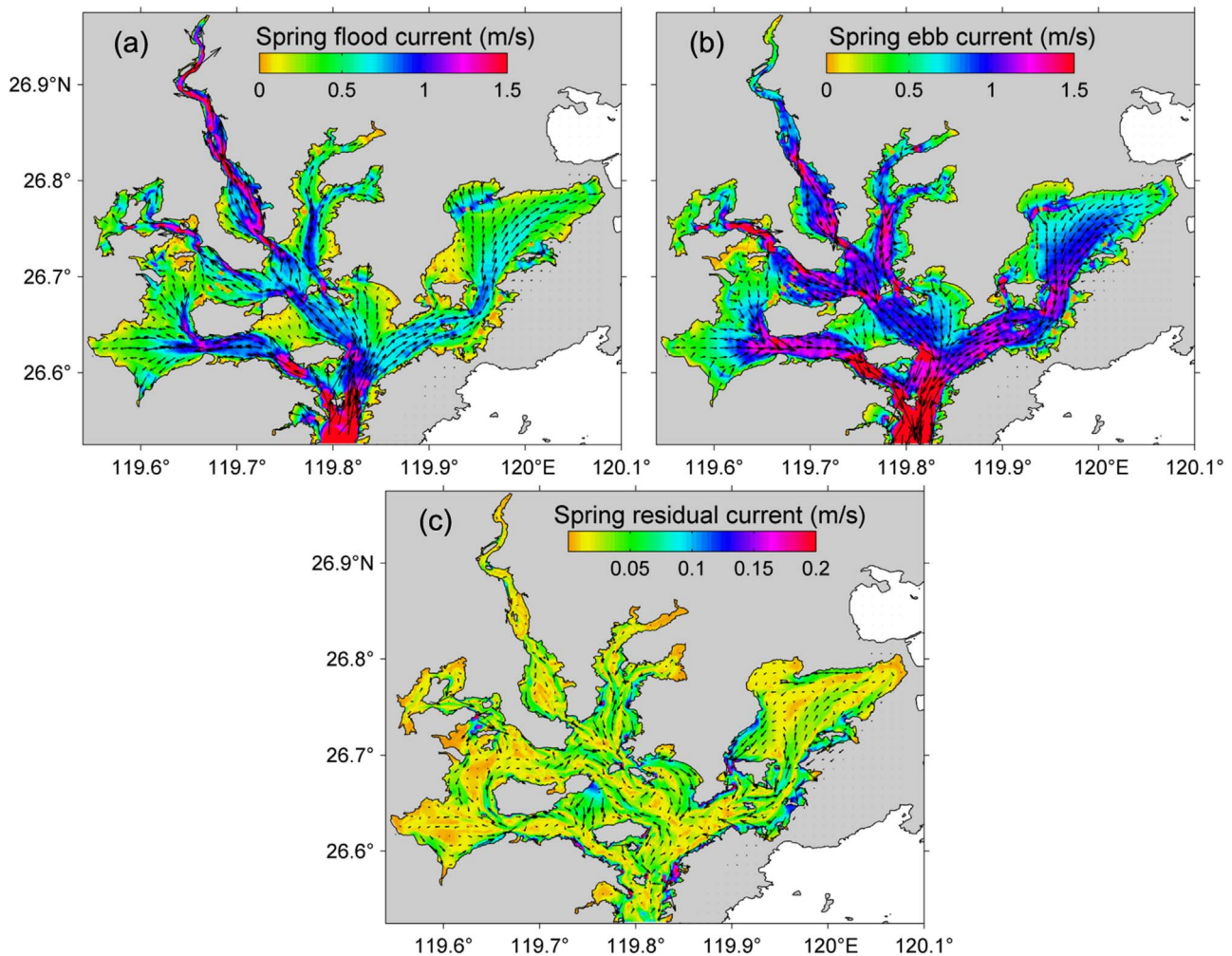
Fig. 8. Simulated flow fields in Sansha Bay during spring tide with color shading denoting current speed (in m s^{-1}) and vectors denoting current direction: (a) flood current, (b) ebb current, and (c) residual current.

areas, or due to the nonlinear interactions between the residual current and the topography. The residual currents do not exhibit a universal direction toward the inner or outer bay, either in the main channels or in tidal flats. This implies that the residual currents have a limited role in water exchange between the bay and the outer waters, and hence the physical based restoration of water quality in Sansha Bay has to rely primarily on tidal currents instead of residual currents.

4.2. Water-exchange capability

The water-exchange capability of Sansha Bay with the open sea is studied in this subsection by examining the half-exchange time (T_h), which refers to the time required for half of the sea water within the bay replaced by sea water from the open sea under the influence of tidal and residual currents. The model (see Section 2.1) is used to calculate the time needed for a pollutant to reduce its concentration to half of its initial value, set to unit, at each node of the model domain.

A set of sensitivity runs are designed to investigate the factors affecting T_h within the bay. Specifically, this includes (i) increasing the runoff of Saijiang River (see Fig. 1 for location; termed as Case 1), (ii) dredging of tidal flats near the bay head regions (Case 2), and (iii) opening up a passage between the open sea and Dongwuyang at its relative narrow eastern boundary (Case 3). A comparison of water depths before and after dredging of the tidal flats is shown in Fig. 9. Basically, dredging is achieved in the model by transforming the "wet-and-dry" cells into "wet" cells. A control run (also termed as Case 0) is

also set up in order to compare with the sensitivity runs. The control run is configured to be the closest to the realistic condition, i.e., without dredging or an extra passage in Dongwuyang. Saijiang River runoff is ignored in the control run because it is normally very small due to the sluice gate control. Specific configurations for the control run and the sensitivities are detailed in Table 1.

The distribution of T_h for the control run (Fig. 10) suggests that T_h in the main channels (< 10 d) is generally shorter than that in bay heads (> 30 d). Sea water in the vicinity of Guanjingyang and Dongchong Channel exchanges at a relatively high rate with the open sea, both with T_h < 5 d. By contrary, sea water in Baima Harbor has a low exchange rate (T_h > 40 d) with the open sea because it has a longest distance to the bay mouth and also that the ebb currents in this harbor are weak without clear outward residual currents (Fig. 8). T_h in the eastern bay head of Dongwuyang also exceeds 40 d, possibly caused by the weak tidal currents and the inward residual currents in this area (Fig. 8).

The distributions of T_h for the three sensitivity runs are shown in Fig. 11. By increasing the Saijiang River runoff (Case 1), it is expected to see a significantly reduced T_h in Baima Harbor. T_h near the northern tip of the harbor decreases from > 40 d to < 5 d (Fig. 11a). The difference of T_h between this sensitivity and the control run (Fig. 11b) indicates a large negative patch in Baima Harbor, as expected, but it also suggests a small increase of T_h in other bay heads (e.g., Yantian Harbor and Dongwuyang). In terms of dredging of the tidal flats (Case 2), an overall decrease of T_h is seen in all bay heads (Fig. 11c–d). This is
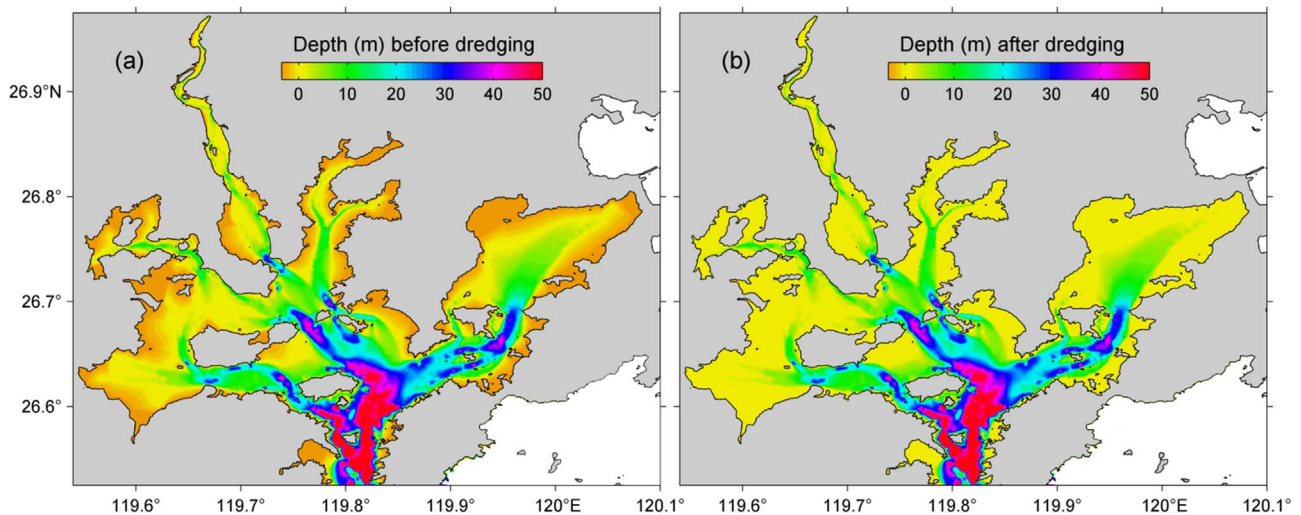
Fig. 9. Comparison of water depths in Sansha Bay (a) before and (b) after dredging of the tidal flats near the bay head regions.

Table 1
Model configurations for the control run and three sensitivity runs.

Case	Saijiang River runoff (m^3 s^{-1})	Tidal flat dredging	Dongwuyang eastern boundary
Case 0 (control run)	0	No	Closed
Case 1	**100**	No	Closed
Case 2	0	**Yes**	Closed
Case 3	0	No	**Open**
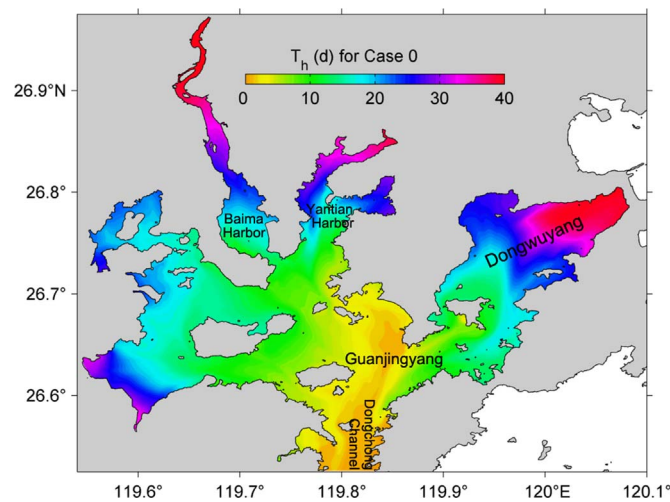
Fig. 10. Distribution of the half-exchange time T_h (see main texts for details) in Sansha Bay.

consistent with the above finding that deeper areas (e.g., main channels) are associated with stronger currents (Fig. 8) and hence a shorter T_h (Fig. 10). By opening up a passage between the open sea and Dongwuyang (Case 3; see the heavy black dash lines in Fig. 11e–f), it is evident that T_h in the entire Dongwuyang decreases dramatically, because under the influence of tides it can now directly exchange water with the open sea through its eastern passage. Nevertheless, there is also a small increase of T_h in other bay heads (e.g., Baima Harbor and Yantian Harbor), similar to the consequences in Case 1.

In a short summary, dredging of tidal flats is most effective in terms of increasing the exchange rate of seawater near bay heads where T_h is relatively long, although it can be imagined that a huge amount of coastal construction is needed in this case. Alternatively, increasing

river runoff or opening up an extra passage is more economically feasible and also significantly enhances the exchange rate locally, but it seems to cause a side effect of slight slowing in the exchange of sea water in other bays with the open sea. Such a remote side effect is probably due to changes in residual currents, although the increments in T_h are mostly minor.

5. Conclusions

Based on the shallow water hydrodynamic finite element model (SHYFEM), a two-dimensional hydrodynamic model has been developed for Sansha Bay in this study, in order to investigate its hydrographic features and in particular the ability to exchange sea water with the open sea. The model is designated to provide a physical background for ecological restoration in this area. The observations collected in Sansha Bay in January-March 2013 are used to validate the water levels and currents simulated by the model. The main results are summarized as follows.

i)   The two-dimensional hydrodynamic model is generally capable of reproducing the variability of water level and currents in Sansha Bay.
ii) Sea water from the open sea flows into Sansha Bay along the main channels during flood tide, and the flow directions reverse during ebb tide. Deeper areas (e.g., main channels) are accompanied by stronger flood/ebb current velocities with a magnitude of approximately 1 m s^{-1}, and even exceeding 1.5 m s^{-1} in the narrow Dongchong Channel. Shallower areas (e.g., tidal flats or bay heads) are accompanied by weaker velocities generally with a magnitude less than 0.5 m s^{-1}. The residual currents are much weaker without a clear inward or outward direction.
iii) The water-exchange ability is examined via the distribution of half-exchange time (T_h) in Sansha Bay. For the present situation, T_h is generally less than 10 d along the main channels, while exceeds one month from tidal flats to bay head areas. Sensitivity runs suggest that (a) dredging of the tidal flats can help increase the exchange rate of seawater near bay heads as a whole, and (b) increasing river runoff or opening up an extra passage can significantly increase the exchange rate locally whereas slightly decrease it in other secondary bays.

In summary, the most economical restoration scheme based on the hydrodynamic features is to take good advantage of the strong tidal currents in Sansha Bay. For example, it would be helpful to discharge sewage in appropriate periods (during ebb tide) and locations (deep
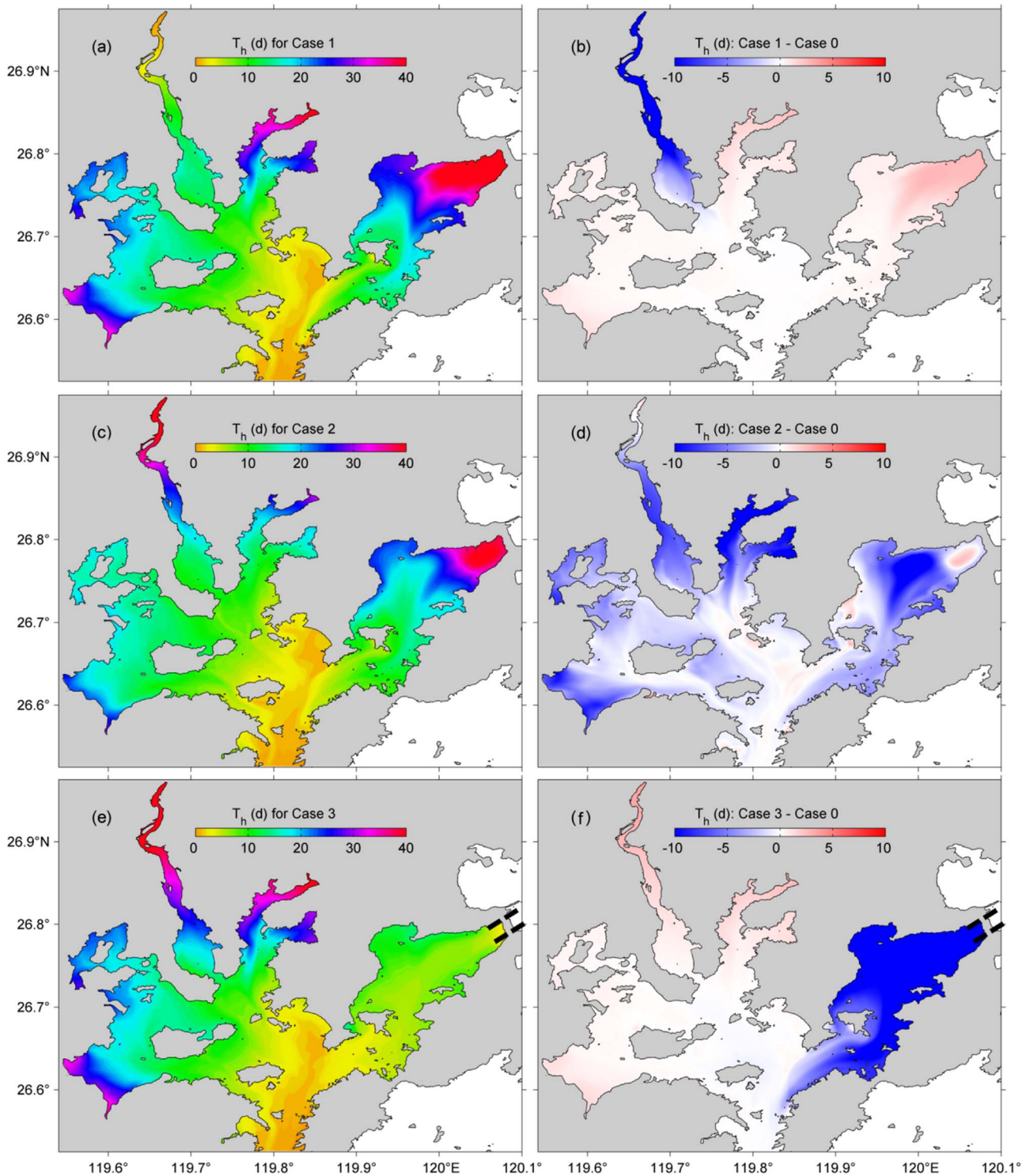
Fig. 11. Distribution of the (left) half-exchange time T_h for the three sensitivity runs and (right) the differences compared with that of the control run.

water areas). The exchange rate can also be enhanced by increasing river runoff, moderate dredging of tidal flats and potentially opening up extra passages to connect with the open sea.

References

Boesch, D.F., Brinsfield, R.B., Magnien, R.E., 2001. Chesapeake Bay eutrophication: scientific understanding, ecosystem restoration, and challenges for agriculture. J. Environ. Qual. 30 (2), 303–320.

Cai, Q., 2007. Study on Maine ecological environment of Sansha Bay in Fujian. Environ. Monit. China 23 (6), 101–105, (in Chinese with English abstract).

Csanady, G.T., 1982. Circulation in the Coastal Ocean. Springer, 279.

Cucco, A., Umgiesser, G., 2006. Modeling the Venice Lagoon residence time. Ecol. Model. 193 (1), 34–51.

Lin, H., An, B., Chen, Z., Sun, Z., Chen, H., Zhu, J., Huang, L., 2016a. Distribution of summertime and wintertime temperature and salinity in Sansha Bay. J. Xiamen Univ. Natur. Sci. 55 (3), 349–356, (in Chinese with English abstract).

Lin, H., Hu, J., Zhu, J., Cheng, P., Chen, Z., Sun, Z., Chen, D., 2016b. Tide- and wind-driven variability of water level in Sansha Bay, Fujian, China. Front. Earth Sci.. http://dx.doi.org/10.1007/s11707-016-0588-x.

Liu, J., Zheng, Q., Chen, H., Yu, Z., Lin, Y., 2003. Water quality condition in Sansha Bay. J. Oceanogr. Taiwan Strait. 22 (2), 201–204, (in Chinese with English abstract).

Shen, L., Li, C., Wu, X., Gong, L., Hao, S., 2014. Temporal and spatial variation characteristics of inorganic nitrogen and active phosphorus and relations with environmental factors in Sansha Bay of Fujian in summer and winter. J. Appl. Oceanogr. 33 (4), 553–561, (in Chinese with English abstract).

Sun, P., Yu, G., Chen, Z., Hu, J., Liu, G., Xu, D., 2015. Diagnostic model construction and example analysis of habitat degradation in enclosed bay: iii. Sansha Bay habitat restoration strategy. Chin. J. Oceanol. Limnol. 33 (2), 477–489. http://dx.doi.org/10.1007/s00343-015-4169-8.

Thompson, K.R., Sheng, J., 1997. Subtidal circulation on the Scotian Shelf: assessing the hindcast skill of a linear, barotropic model. J. Geophys. Res. 102, 24987–25003. http://dx.doi.org/10.1029/97JC00368.

Umgiesser, G., 2009. SHYFEM: Finite Element Model for Coastal Seas – User Manual. Venezia.ISMAR-CNR, 38pp.

Umgiesser, G., Canu, D.M., Cucco, A., Solidoro, C., 2004. A finite element model for the Venice Lagoon. Development, set up, calibration and validation. J. Mar. Syst. 51, 123–145.

Urrego-Blanco, J., Sheng, J., 2012. Interannual variability of the circulation over the eastern Canadian shelf. Atmos. Ocean. 50, 277–300. http://dx.doi.org/10.1080/07055900.2012.680430.

Wang, C., Sun, Q., Jiang, S., Wang, J., 2011. Evaluation of pollution source of the bays in Fujian Province. Procedia Environ. Sci. 10, 685–690.

Wang, Y., Wang, C., Song, Z., 2002. Impacts of Tieji Bay reclamation project on deep channel at Sansha Bay. J. Hohai Univ. Natur. Sci. 30 (6), 99–101, (in Chinese with English abstract).

Wang, Y., Song, Z., Jiang, C., Kong, J., Liu, Q., 2009. Numerical and Environmental Studies of Bays in Fujian Province – Sansha Bay (in Chinese). Ocean Press, Beijing, 283.

Wu, H.Y., Chen, K.L., Chen, Z.H., Chen, Q.H., Qiu, Y.P., Wu, J.C., Zhang, J.F., 2012. Evaluation for the ecological quality status of coastal waters in East China Sea using fuzzy integrated assessment method. Mar. Poll. Bull. 64, 546–555.

Ye, H., Wang, Y., Cao, B., 2007. Tidal prism of Sansha Bay and its water exchange with the open sea. J. Hohai Univ. Natur. Sci. 35 (1), 96–98, (in Chinese with English abstract).

Zhang, H., Sheng, J., 2013. Estimation of extreme sea levels over the eastern continental shelf of North America. J. Geophys. Res. 118, 6253–6273. http://dx.doi.org/10.1002/2013JC009160.

Zhang, H., Sheng, J., 2015. Examination of extreme sea levels due to storm surges and tides over the northwest Pacific Ocean. Cont. Shelf Res. 93, 81–97. http://dx.doi.org/10.1016/j.csr.2014.12.001.